



Published in final edited form as:

*Osteoarthritis Cartilage*. 2020 July ; 28(7): 977–987. doi:10.1016/j.joca.2020.04.002.

## An altered heparan sulfate structure in the articular cartilage protects against osteoarthritis

A.-C. Severmann<sup>†,a</sup>, K. Jochmann<sup>†,a</sup>, K. Feller<sup>†</sup>, V. Bachvarova<sup>†</sup>, V. Piombo<sup>†</sup>, R. Stange<sup>||</sup>, T. Holzer<sup>‡</sup>, B. Brachvogel<sup>‡</sup>, J. Esko<sup>§</sup>, T. Pap<sup>||</sup>, D. Hoffmann<sup>¶</sup>, A. Vortkamp<sup>†,\*</sup>

<sup>†</sup>Department of Developmental Biology, Center for Medical Biotechnology, Faculty Biology, University Duisburg-Essen, Germany

<sup>‡</sup>Center for Biochemistry, Department of Pediatrics and Adolescent Medicine, Experimental Neonatology, Medical Faculty, University of Cologne, Germany

<sup>§</sup>Department of Cellular and Molecular Medicine, Glycobiology Research & Training Center, University of California, San Diego, La Jolla, CA, 92093-0687, USA

<sup>||</sup>Zentrum für Muskuloskelettale Medizin, Westfälische Wilhelms-Universität Münster, Germany

<sup>¶</sup>Department Bioinformatics and Computational Biophysics, Center for Medical Biotechnology, Faculty Biology, University Duisburg-Essen, Germany

### SUMMARY

**Objective:** Osteoarthritis (OA) is a progressive degenerative disease of the articular cartilage caused by an unbalanced activity of proteases, cytokines and other secreted proteins. Since

---

This is an open access article under the CC BY-NC-ND license (<http://creativecommons.org/licenses/by-nc-nd/4.0/>).

\*Address correspondence and reprint requests to: A. Vortkamp, Department of Developmental Biology, Center for Medical Biotechnology, Faculty Biology, University Duisburg-Essen, 45117, Essen, Germany. [andrea.vortkamp@uni-due.de](mailto:andrea.vortkamp@uni-due.de) (A. Vortkamp).

Author contribution

Conception and design: ACS, KJ, AV.

Analysis and interpretation of the data: ACS, KJ, DH, AV.

Drafting of the article: ACS, AV.

Critical revision of the article for important intellectual content: ACS, KJ, VB, VP, RS, BB, JE, TP, DH, AV.

Final approval of the article: ACS, KJ, DH, AV.

Statistical expertise: DH.

Obtaining of funding: AV, BB.

Administrative, technical, or logistic support: KF, TH, RS.

Collection and assembly of data: ACS, KJ, KF, VB.

<sup>a</sup>Equal contribution.

Animal experiments

All animal experiments were carried out according to the institutional guidelines of the University of Duisburg-Essen and approved by the animal welfare officer. Mouse husbandry was approved by the city of Essen (Az: 32-2-11-80-71/348) in accordance with § 11 (1) 1a of the “Tierschutzgesetz”. Work with transgenic animals was approved by the “Bezirksregierung Düsseldorf” (Az: 53.02.01-D-1.55/12, Anlagen-Nr. 1,464) in accordance with § eight Abs. four Satz two of the “Gentechnikgesetz”.

The induction of Cre-recombination by doxycycline administration was approved by the “Landesamt für Natur, Umwelt und Verbraucherschutz (LANUV) Nordrhein-Westfalen” (Az: 84–02.05.20.12.156), as well as the surgical induction of OA (Az: 84–02.04.2011A280).

Conflict of interest

The authors declare no conflicts of interest.

Supplementary data

Supplementary data to this article can be found online at <https://doi.org/10.1016/j.joca.2020.04.002>.

heparan sulfate (HS) determines the activity of many extracellular factors, we investigated its role in OA progression.

**Methods:** To analyze the role of the HS level, OA was induced by anterior cruciate ligament transection (ACLT) in transgenic mice carrying a loss-of-function allele of *Ext1* in clones of chondrocytes (*Col2-rtTA-Cre;Ext1<sup>e2fl/e2fl</sup>*). To study the impact of the HS sulfation pattern, OA was surgically induced in mice with a heterozygous (*Ndst1<sup>+/-</sup>*) or chondrocyte-specific (*Col2-Cre;Ndst1<sup>fl/fl</sup>*) loss-of-function allele of the sulfotransferase *Ndst1*. OA progression was evaluated using the OARSI scoring system. To investigate expression and activity of cartilage degrading proteases, femoral head explants of *Ndst1<sup>+/-</sup>* mutants were analyzed by qRT-PCR, Western Blot and gelatin zymography.

**Results:** All investigated mouse strains showed reduced OA scores (*Col2-rtTA-Cre;Ext1<sup>e2fl/e2fl</sup>*: 0.83; 95% HDI 0.72–0.96; *Ndst1<sup>+/-</sup>*: 0.83, 95% HDI 0.74–0.9; *Col2-Cre;Ndst1<sup>fl/fl</sup>*: 0.87, 95% HDI 0.76–1). Using cartilage explant cultures of *Ndst1* animals, we detected higher amounts of aggrecan degradation products in wildtype samples (NITEGE 4.24-fold, 95% HDI 1.05–18.55; VDIPEN 1.54-fold, 95% HDI 1.54–2.34). Accordingly, gelatin zymography revealed lower Mmp2 activity in mutant samples upon RA-treatment (0.77-fold, 95% HDI: 0.60–0.96). As expression of major proteases and their inhibitors was not altered, HS seems to regulate cartilage degeneration by affecting protease activity.

**Conclusion:** A decreased HS content or a reduced sulfation level protect against OA progression by regulating protease activity rather than expression.

## Keywords

Heparan sulfate; Osteoarthritis; *Ndst1*; *Ext1*; Aggrecan degradation; Mmp2; Articular cartilage

## Introduction

The mechanical properties of the articular cartilage are determined by a network of collagen fibers providing tensile strength, and glycosaminoglycans (GAGs), predominantly chondroitin sulfate (CS) and hyaluronic acid, giving the tissue its compressive features. This extracellular matrix (ECM) undergoes slow but constant remodeling. During osteoarthritis (OA), the balance between ECM synthesis and degradation shifts towards catabolic processes, including the degradation of collagens and aggrecan by members of the matrix metalloproteinase (MMP) and a disintegrin and metalloproteinase with thrombospondin motifs (ADAMTS) families<sup>1</sup>.

The distribution and activity of many secreted proteins like proteases, cytokines and growth factors are regulated by heparan sulfate (HS) carrying proteoglycans (HSPGs)<sup>2,3</sup>. The synthesis of the HS chain takes place in the Golgi apparatus where the glycosyltransferases EXT1 and EXT2 catalyze the elongation of the polysaccharide chain by adding alternating units of D-glucuronic acid (GlcA) and N-acetyl-D-glucosamine (GlcNAc) to a tetrasaccharide linker attached to serine residues of the core proteins. Simultaneously, the sugar chain is modified by N-deacetylase-N-sulfotransferases (NDST1–4), the D-glucuronyl-C5-epimerase (GLCE), and several 2-O, 3-O and 6-O sulfotransferases. The overlapping expression of these enzymes generates a tissue-specific sulfation pattern, which determines the binding

affinities of HS to extracellular proteins and thereby their activity and distribution in the ECM<sup>4</sup>.

To gain insight into the importance of HS for the regulation of articular cartilage homeostasis, we have investigated the progression of OA in three mouse strains carrying mutations in either *Ext1* or *Ndst1*. While homozygous deletion of *Ext1*, which results in a complete loss of HS, is embryonically lethal<sup>5</sup>, mice carrying a chondrocyte-specific, clonal deletion of *Ext1* (*Col2-rtTA-Cre;Ext1<sup>e2fl/e2fl</sup>*) are viable and fertile<sup>6</sup>. These mice have been created to mimic the human Multiple Osteochondroma syndrome, which originates in mutations in *EXT1* or *EXT2*<sup>7,8</sup>. Interestingly, while HS-deficient chondrocytes at the border of the growth plate develop into osteochondromas<sup>6,9,10</sup>, mutant cells in the articular cartilage morphologically resemble hypertrophic chondrocytes (personal observation and<sup>11</sup>). Since the presence of hypertrophic chondrocytes in the articular cartilage has been described as an early sign of OA<sup>12-14</sup>, we hypothesized that *Col2-rtTA-Cre;Ext1<sup>e2fl/e2fl</sup>* mutants are prone to develop OA.

In contrast to *Ext1* deficiency the inactivation of *Ndst1* (*Ndst1<sup>-/-</sup>*), which determines regions of high sulfation on the HS chain, results in the production of severely undersulfated HS<sup>15,16</sup>. Homozygous *Ndst1<sup>-/-</sup>* mutants die perinatally due to respiratory failure, while heterozygous *Ndst1<sup>+/-</sup>* animals are viable and do not show any obvious phenotypic alterations. Nevertheless, mild changes in the HS structure have been described<sup>15</sup>, which may become important during ageing or under stress.

In this study, we show that *Col2-rtTA-Cre;Ext1<sup>e2fl/e2fl</sup>* mice develop reduced OA during ageing and after surgical induction of OA. Similarly, heterozygous and chondrocyte-specific inactivation of *Ndst1* lead to less severe OA. Using femoral head explants, we demonstrate that aggrecan and collagen degradation are reduced in the articular cartilage of *Ndst1<sup>+/-</sup>* mutants and identify MMP2 as a protease with decreased proteolytic activity.

## Methods

### Transgenic mice

Transgenic *Col2-rtTA-Cre;Ext1<sup>e2fl/e2fl</sup>* [Tg(Col2a1-rtTA,tetO-cre) 22Pjro; Ext1<sup>tm1.1Ves</sup>]<sup>6</sup>, *R26R-LacZ* [Gt(ROSA)26Sor<sup>tm1Sor</sup>]<sup>17</sup>; *Ndst1<sup>fl/fl</sup>* mice [Ndst1<sup>tm1Grob</sup>]<sup>15</sup>, *Prrx1-Cre* [Tg(Prrx1-cre)1Cjt]<sup>18</sup> and *Col2-Cre* [Tg(Col2a1-cre)1Star]<sup>19</sup> mice were maintained on a C57Bl/6J genetic background. Up to six females, one breeding pair or single males were kept in air filtered cages (SPF conditions, Green Line, Techniplast) under a 12 h light/dark cycle on regular bedding with nesting material (Abed) as environmental enrichment and food (Sniff) and water ad libidum.

Genotyping was performed by PCR on tail tip DNA (DirectPCR Lysis Reagent; VIAGEN) with primers listed in Table S1. Allele recombination in *Col2-rtTA-Cre;Ext1<sup>e2fl/e2fl</sup>* mice was induced by peritoneal injection of 80 mg Doxycycline per kg body weight (kgbw) into lactating dams at postnatal day 8 (P8)<sup>6</sup>. Mice undergoing surgery received 1 mg/kgbw Doxycycline at 6 weeks.

## Surgical induction of OA

OA was induced in the left knee of female mice (8 weeks; approximately 20 gbw) by anterior cruciate ligament transection (ACLT<sup>20,21</sup>). As a control (sham) the joint capsule of the contralateral leg was incised. Mice were anesthetized with 160 mg Ketamine and 8 mg Xylazine/kgbw. Carprofen (5 mg/kgbw) was provided perioperatively and 3 days post-surgery. Health status was controlled daily. Litters with at least two mutant and control mice were operated in a blinded manner on the same day and caged together. Information about litters and operation groups were included in the statistical evaluation.

## Histology

For the histological analysis, knees were dissected, fixed in 4% paraformaldehyde, decalcified in 25% EDTA and embedded in paraffin. 7 µm Sections were stained with Safranin-O. OA was evaluated on frontal sections according to the OARSI-scoring system in a double blinded manner<sup>22</sup>. Mean scores of the four quadrants of the femoro-tibial joint are displayed. Articular cartilage thickness was measured on frontal sections using ImageJ software<sup>23</sup>. Immunofluorescence analysis was performed with mouse anti-collagen type X (Hybridoma), rabbit anti-aggrecan (Millipore) and corresponding secondary antibodies (Jackson ImmunoResearch, ThermoFisher)<sup>24</sup>. β-Galactosidase was detected as described<sup>10</sup>.

## Expression analysis by qRT-PCR

qRT-PCR was performed on femoral head cDNA (RNeasy Lipid tissue Kit, QIAGEN; Maxima First Strand Kit, Fermentas) with the StepOnePlus Real-Time PCR (ThermoFisher Scientific) or CFX96 Touch Real-Time PCR System (BioRad) using EVA Green PCR Master Mix (BioBudget) and primers listed in Table S2.

## Aggrecan degradation

Aggrecan degradation was investigated as described<sup>25</sup>. In brief, femoral heads of 4 weeks old mice were cultured pairwise in medium without and with 10 µM retinoic acid (RA) for 3 days. The GAG concentrations of the culture supernatant, a guanidium hydrochloride (GuHCl) extract of the femoral head and a papain digest of the remaining tissue were determined by dimethylmethylene blue assay to estimate total aggrecan content. Samples from at least two littermates with the same genotype were pooled, dialyzed and freeze-dried. The re-dissolved samples were digested with Chondroitinase ABC (Sigma) and analyzed by Western Blot for VDIPEN and NITIGE neo-epitopes. Signal intensity was quantified against total aggrecan content and background signal of the respective blot.

## Western Blot

The following antibodies were used: for MMP and ADAMTS activity: anti-VDIPEN<sup>26</sup>, and rabbit anti-NITEGE (Polyclonal rabbit α-aggrecan neo (NITEGE) IgG, Thermo Scientific) and the respective IRdye680RD secondary antibody (LI-COR); for MMP2 protein: Rat anti-MMP2 (Chemicon), biotinylated goat anti-rabbit IgG (Vector Laboratories) and IRdye 800CW Streptavidin (LI-COR). Signal detection was performed with Odyssey CLx (LI-COR).

## MMP activity

For gelatin zymography recombinant mouse/rat MMP2 (rMMP2, R&D systems) or supernatants of femoral head cultures were separated on 8% SDS PAGE gels containing 0.1% gelatin. Renaturation, digestion and staining were carried out as described<sup>27</sup>. Degradation bands were quantified with Photoshop CS 4 (Adobe) or ImageStudioLite (LICOR) software.

## Statistical analysis

To estimate the effects of genotype, age, and other predictors on measured response quantities such as cartilage thickness, zymogram signals, etc. we described the relations between the responses and predictors as hierarchical generalized linear models (GLMs)<sup>28</sup>, with the exception of the response OA scores, for which we used a beta regression (see Supplementary Information). Strictly positive response quantities (except OA scores) were log-transformed for this analysis to enable use of Gaussian noise distributions for the transformed response<sup>29</sup>. OA scores were normalized to range 0–1. Weakly informative prior distributions were assumed for the slopes and intercepts of the GLMs, as proposed by R-package rstanarm, version 2.17.4 (<https://CRAN.R-project.org/package=rstanarm>; details in Supplementary Information).

Between groups of related measurements, e.g., measurements for animals of the same litter, intercepts were allowed to vary according to a joint noise distribution, constituting a second level of our hierarchical probability models. The posteriors of the probability models were numerically inferred by Bayesian analysis with rstanarm<sup>30</sup>. The agreement of the models with reality was checked by graphical posterior predictive checks (PPCs), i.e., comparisons of response distributions simulated with the fitted model vs distributions of actual measurements. If deviations in the PPCs were observed, the model was modified, typically by including an interaction, as e.g., in the case of the log cartilage thickness. If several models were considered for the same response, the best model was identified by comparing the competing models with respect to their ability to generalize to unseen data in an approximate leave-one-out cross-validation<sup>31</sup>.

Detailed information on the statistical outcomes and the number of animals used in each experiment can be found in Tables S3 and S4.

## Results

### Clonal deletion of *Ext1* in chondrocytes protects from OA

To investigate the role of HS in the maintenance of the articular cartilage, we aged *Col2-rtTA-Cre;Ext1<sup>e2fl/e2fl</sup>* mice after recombination of the allele at postnatal day 8 (P8). Introduction of a *R26R-LacZ* reporter allele (*Col2-rtTA-Cre;Ext1<sup>e2fl/e2fl</sup>;R26R-LacZ*) identified clusters of mutant, hypertrophic-appearing cells, which are surrounded by wildtype articular cartilage [Fig. 1(A)]. Since hypertrophic chondrocytes in the articular cartilage are regarded as a sign of early OA<sup>12–14</sup>, we investigated OA development in knee joints of 3, 6, 12 and 18 month old mice using the OARSI scoring system<sup>22</sup>. No obvious signs of OA were detected in 3 month (3m) old wildtype or *Col2-rtTA-Cre;Ext1<sup>e2fl/e2fl</sup>* mice

(mean OARSI scores 3m: 0.32 and 0.17, respectively), while at 6m and 12m first signs of cartilage degeneration were observed in both genotypes (OARSI scores 6m: 0.83 and 0.73; 12m: 1.10 and 1.10). At 18m control mice displayed mild to moderate signs of OA (OARSI score: 2.17) [Fig. 1(B)]. Surprisingly, at this stage *Col2-rtTA-Cre;Ext1<sup>e2fl/e2fl</sup>* mutants did not develop the expected increased signs of OA, but seemed to develop less OA (OARSI score 0.67). There was a clear positive effect of age on the observed OA scores (increase over time: 0.13 OARSI score units per month; 95% highest density intervals (HDI) 0.08–0.18). Importantly, OA scores of mutant mice increased less than those of their wildtype littermates (mean increase factor: –0.09, 95% HDI –0.16 to –0.03; Tables S3 and S4).

At all analyzed time points, the observed clusters of enlarged, mutant cells in the articular cartilage did not obviously change in morphology, number or size [Fig. 1(D)]. Safranin-O and immunofluorescence staining for aggrecan on sections of P28 mice showed that these clusters were surrounded by a thick, proteoglycan-rich matrix containing increased levels of aggrecan [Fig. 1(E)]. The loss of HS seems thus to alter the ECM composition surrounding the HS-deficient cells. To further characterize the mutant cells, we analyzed the expression of the hypertrophy marker Collagen type X (COLX) by immunofluorescence. Although COLX was clearly present in the growth plate, we could not detect COLX in mutant or wildtype articular chondrocytes of the same section indicating that, although enlarged, the HS-deficient cells are molecularly distinct from hypertrophic chondrocytes of the growth plate [Fig. 1(F)].

To confirm the role of HS in OA pathogenesis, we surgically induced OA in *Col2-rtTA-Cre;Ext1<sup>e2fl/e2fl</sup>* mutants by ACLT<sup>20,21</sup> at 8 weeks of age after recombining the *Ext1* allele at 6 weeks. At 12 weeks, knee joints were dissected and Safranin-O stained frontal sections were scored for OA. As expected, control littermates developed severe signs of OA, while reduced scores were observed in *Col2-rtTA-Cre;Ext1<sup>e2fl/e2fl</sup>* mutants (mean OARSI scores: 3.8, and 3.3; median reduction factor of 0.83; 95% HDI 0.72–0.96; Fig. 1(C), Tables S3 and S4). Sham-operated contralateral legs showed no signs of OA pointing against a systemic effect of the operation or a substantial shift in weight bearing (OARSI scores: 0.19 (*Ext1<sup>e2fl/e2fl</sup>*) and 0.28 (*Col2-rtTA-Cre;Ext1<sup>e2fl/e2fl</sup>*)). In summary, the surgical model confirmed the findings observed in aged mice indicating that the HS level affects the severity of OA.

### Ndst1-mutant mice display reduced OA progression

Since the clonal inactivation of *Ext1* in *Col2-rtTA-Cre;Ext1<sup>e2fl/e2fl</sup>* mice makes it difficult to investigate the overall function of HS during OA pathogenesis, we analyzed OA progression in mice carrying a heterozygous loss-of-function allele of *Ndst1*. We surgically induced OA in control and *Ndst1<sup>+/-</sup>* mice at 8 weeks of age and analyzed the femorotibial joints as described. Sham-operated knees showed no obvious signs of cartilage erosion (mean OARSI scores: 0.11 and 0.17). In contrast, the ACLT-operated joints displayed severe OA including loss of the articular surface lamina and severe erosion of the articular cartilage occasionally reaching the subchondral bone [Fig. 2(A)]. We found reduced OA progression in heterozygous *Ndst1<sup>+/-</sup>* mice compared to controls (OARSI scores: 2.9 and 3.6; median reduction factor: 0.82, 95% HDI 0.74–0.90; Fig. 2(B), Tables S3 and S4). To evaluate



whether complete loss of *Ndst1* might have a similarly protective effect, we investigated mice carrying a chondrocyte-specific deletion of *Ndst1* (*Col2-Cre;Ndst1<sup>fl/fl</sup>*). In contrast to the strong phenotypes seen in *Ndst1<sup>-/-</sup>* animals, *Col2-Cre;Ndst1<sup>fl/fl</sup>* mice were viable and fertile, and displayed no obvious morphological alterations of the skeleton. Sham surgery did not trigger OA development in *Ndst1<sup>fl/fl</sup>* or *Col2-Cre;Ndst1<sup>fl/fl</sup>* animals (OARSI scores: 0.05 and 0.12), while surgical induction led to severe OA (OARSI scores: 3.4 and 3.0; Fig. 2(A) and (B)). As observed for the *Ndst1<sup>+/-</sup>* mutants, the genotype had a modest, but clearly negative effect on OA progression in *Col2-Cre;Ndst1<sup>fl/fl</sup>* mice (median reduction factor 0.87, 95% HDI 0.76–1.00; Tables S3 and S4).

### Chondrocyte-specific loss of *Ndst1* alters joint morphology

During the histological evaluation of *Col2-Cre;Ndst1<sup>fl/fl</sup>* knees we noticed morphological changes of the articular cartilage [Fig. 2(C)]. Analysis at 1, 3 and 18 months of age revealed an increased thickness in *Col2-Cre;Ndst1<sup>fl/fl</sup>* mutants at all investigated time points (1m: 131  $\mu$ m and 104  $\mu$ m; 3m: 109  $\mu$ m and 95  $\mu$ m; 18m: 108  $\mu$ m and 100  $\mu$ m; mean increase in thickness: 1.24-fold; 95% HDI 1.15–1.33; Fig. 2(D), Tables S3 and S4). An increased articular cartilage thickness might contribute to the reduced OA scores by delaying the complete erosion of the cartilage down to the subchondral bone. We did, however, not detect differences in articular cartilage thickness in heterozygous *Ndst1<sup>+/-</sup>* mutants (data not shown), which are also protected against OA. This indicates that additional degenerating mechanisms are regulated by the altered HS structure.

### Expression of ECM-degrading proteases is unaltered in *Ndst1<sup>+/-</sup>* mice

To test if the expression of main proteases of the articular cartilage is affected by the altered HS structure, we analyzed the expression of *Mmp2*, *Mmp3*, *Mmp9*, *Mmp13*, *Adams4* and *Adams5*<sup>1,32,33</sup> in *Ndst1<sup>+/-</sup>* femoral head cultures treated with RA to induce cartilage degradation<sup>34</sup> by qRT-PCR. We did not detect differences in the expression of any of the proteases between *Ndst1<sup>+/-</sup>* mutants and wildtype littermates (Fig. 3(A); Tables S3 and S4). On the activity level, MMPs are controlled by members of the tissue inhibitor of metalloproteinases (TIMP) family<sup>35</sup>. We thus quantified the expression of *Timp1*, *Timp2* and *Timp3* in the same RNA samples, but did not detect differences in their expression between *Ndst1<sup>+/-</sup>* mutants and controls (Fig. 3(B); Tables S3 and S4).

### Aggrecan degradation is decreased in *Ndst1<sup>+/-</sup>* cartilage explants

Since HS regulates the activity of many extracellular proteins, we next asked if protease function is altered by changes in the HS structure. The degradation of aggrecan by metalloproteases of the ADAMTS and MMP families results in the generation of the neo-epitopes VDIPEN<sup>36</sup> and NITEGE<sup>37</sup>, respectively. To investigate aggrecan degradation, we cultured femoral heads of 4 weeks old *Ndst1<sup>+/-</sup>* and *Ndst1<sup>+/-</sup>* mice and treated them with RA<sup>34</sup>. The presence of each neo-epitope was analyzed in the culture medium and in GuHCl extracts of the explant tissue by Western Blot<sup>25</sup>. In the supernatant of untreated femur heads, VDIPEN and NITEGE neo-epitopes were only detected in few samples. Higher levels of both epitopes were present in GuHCl extracts of these tissues, but the signal intensity could not always be quantified [Fig. 4(A) and (B)]. Nevertheless, the obtained data hint at decreased levels of NITEGE neo-epitopes in *Ndst1<sup>+/-</sup>* samples. After RA treatment, both

neo-epitopes could reproducibly be detected in the culture medium and GuHCl extracts. In accordance with the elevated OA scores higher levels of aggrecan degradation products were found in the supernatants (VDIPEN: 1.43-fold; NITEGE: 2.13-fold) and tissue extracts of wildtype mice (VDIPEN: 1.52-fold; NITEGE: 2.50-fold) [Fig. 4(A) and (B)]. Taken together, there was a clear effect of the genotype on the detected VDIPEN and NITEGE signals after RA treatment (wildtype-associated mean increases VDIPEN: 1.54; 95% HDI 1.00–2.34; NITEGE: 4.24; 95% HDI 1.05–18.6; Tables S3 and S4).

### MMP2 activity is controlled by extracellular proteoglycans

As aggrecan degradation is reduced in *Ndst1*<sup>+/-</sup> mice, we wondered whether the digestion of collagens by MMPs is also affected. Analysis of MMP activity in the supernatant of femoral head cultures by gelatin zymography<sup>38,39</sup> revealed two prominent degradation bands [Fig. 4(C)]. The larger protease of around 65 kDa was also present in the fetal calf serum (FCS)-containing culture medium, while the smaller enzyme of around 58 kDa was specifically detected in the femoral head explants. Zymography using the supernatant of serum-free explant cultures confirmed that the larger degradation signal was caused by the FCS-containing medium, while the ~58 kDa protease was specific for the cartilage explants [Fig. 4(E)]. Without RA, no difference in protease activity could be detected under either culture condition between *Ndst1*<sup>+/-</sup> and control samples (combined median effect factor 1.09, 95% HDI 0.90–1.34; Fig. 4(D), Tables S3 and S4). Importantly, after RA treatment the activity of the ~58 kDa protease was reduced in *Ndst1*<sup>+/-</sup> samples (combined median factor: 0.77, 95% HDI 0.60–0.96; Fig. 4(D), Tables S3 and S4). Additionally, we found a second pair of degradation bands of ~100 kDa under serum-free conditions. The smaller degradation signal was hardly detectable in untreated cultures, but was clearly induced by RA treatment. Again, *Ndst1*<sup>+/-</sup> mutants showed a decreased activity of this protease (mean reduction factor: 0.69, 95% HDI: 0.44–1.14; Fig. S1, Tables S3 and S4).

Considering the sizes of proteases typically found in cartilage, the two enzymes likely represent activated MMP2 (58 kDa) and MMP9 (82 kDa)<sup>40,41</sup>. The presence of MMP2 in the zymogram was confirmed by comparison of the activity bands from supernatants of femur head cultures with recombinant mouse/rat MMP2 (rMMP2; Fig. 4(E)). Furthermore, we detected MMP2 in the supernatant of femoral head explants by Western Blot analysis [Fig. 4(F)].

## Discussion

In this study, we investigated the role of HS during OA pathogenesis and found that reduced HS levels and sulfation attenuated OA development. We demonstrate that the altered HS composition in *Ndst1*<sup>+/-</sup> mutants leads to a reduced degradation of aggrecan and collagens by metalloproteases and identify MMP2 as one protease with altered activity.

Similar to our results, mice lacking the HS-carrier Syndecan 4 (Sdc4) show reduced OA progression after surgical OA induction. Accordingly, increased expression of Sdc4 has been found in OA samples of human patients and rats upon forced exercise, and administration of a Sdc4-specific antibody decreased OA progression in a surgical OA model<sup>42</sup>. Other studies found reduced OA progression in mice lacking the HS-carrying exon three of Perlecan



(*Hspg2*<sup>3-/3-</sup>;43) and lower numbers of osteophytes in mice lacking Perlecan in all joint tissues except for cartilage<sup>44</sup>. These results strongly support our hypothesis that reduced HS levels inhibit the progression of OA.

While inactivation of *Sdc4*, *Perlecan* or *Ext1* decreases the HS level, inactivation of *Ndst1* leads to severely reduced N-, 6-O and 2-O-sulfation of the HS chain<sup>15</sup>. The lower OA scores detected in both *Ndst1* mutants indicate that not only the HS level but also the sulfation pattern affect the integrity of the articular cartilage. This finding is substantiated by analyses of mice lacking the secreted endosulfatases Sulf1 or Sulf2, which remove 6-O sulfate groups from HS chains. Both mutants developed more severe OA upon ageing and after surgery<sup>45</sup>. Furthermore, injection of recombinant Sulf1 into knee joints of wildtype mice reduced surgically induced OA progression<sup>46</sup>, further supporting a protective effect of decreased HS sulfation.

Interestingly, a recent comprehensive study analyzing the expression of 13 core proteins and 25 enzymes of the HS biosynthesis pathway in healthy and osteoarthritic human cartilage revealed that 45% of the investigated genes, including *EXT1* and *NDST1*, showed an increased expression in OA tissues<sup>47</sup>. Furthermore, the degree of 6-O sulfation was increased in the OA samples, supporting a role of the HS structure as a critical regulator of OA progression also in humans.

As outlined above, HS regulates the distribution and activity of many secreted proteins. While an effect on cytokine and growth factor signaling cannot be ruled out, our results strongly support a reduced activity of ADAMTS and MMP proteases in *Ndst1*<sup>+/-</sup> mutants and identify MMP2 as one enzyme with reduced activity. Previous studies revealed that the expression of *Mmp13* and *Adamts5* is increased in the OA cartilage of Sulf1- and Sulf2-deficient mice<sup>45</sup>. In contrast, we could not detect altered expression levels of major cartilage-degrading metalloproteases or their inhibitors in *Ndst1*<sup>+/-</sup> mutants, strongly pointing to a post-transcriptional regulation of protease activity.

To test if the activity of MMP2 is directly regulated by HS, we investigated its physical interaction with HS isolated from E16.5 mouse embryos by affinity chromatography but could not detect evidence for binding (data not shown). This is in contrast to a recent study based on activity assays and molecular modeling, which proposed the formation of MMP2-TIMP3-HS ternary complexes<sup>48</sup>. However, these experiments were based on the addition of HS to *in vitro* formed complexes and the subsequent analysis of MMP activity, while the interaction of HS and MMP2 was not directly addressed.

Our experiments show that not only the activity of MMP2 but also MMP9 and not yet identified members of the ADAMTS family are downregulated in *Ndst1*<sup>+/-</sup> mutants. The regulation of multiple proteases strongly points to a superordinate mechanism. This might include the HS-dependent regulation of activating proteases like MMP14, which activates MMP2<sup>49</sup>, or MMP2, which in turn activates MMP9<sup>50</sup>, or inhibitors of the TIMP family, which regulate different proteases<sup>51</sup>.

Besides reduced enzyme activity the degradation process is likely also affected by an altered structure or an increased thickness of the articular cartilage as seen in *Col2-Cre;Ndst1*<sup>fl/fl</sup>

mutants. Although an increased thickness was not detected in *Ndst1*<sup>+/-</sup> mutants, subtle alterations might contribute to the decreased OARSI scores.

One surprising result of our experiments was that the enlarged, HS-deficient cells in the articular cartilage of *Col2-rtTA-Cre;Ext1*<sup>e2fl/e2fl</sup> mice did not advance OA progression. Analysis of COLX expression demonstrated that the mutant cells do not resemble hypertrophic chondrocytes of the growth plate. Morphological hypertrophy therefore does not necessarily reflect a distinct differentiation status. The *Ext1*-deficient cells are surrounded by a dense, Safranin-O-positive ECM, which contains increased amounts of perlecan<sup>11</sup> and aggrecan. An increase in ECM production has also been observed after treatment of chondrocytes with heparanase or the HS antagonist Surfen<sup>52-54</sup>. Furthermore, in a parallel study we demonstrate that mice with a severely decreased HS-content (*Ext1*<sup>gt/gt</sup>) or an altered sulfation pattern (*Hs2st1*<sup>-/-</sup>) show increased levels of CS, mostly bound to aggrecan<sup>55</sup>. The upregulation of CS-carrying proteoglycans and other ECM components might thus be a common compensatory reaction of chondrocytes to an altered HS structure and might contribute to an improved quality of the articular cartilage.

While our data identify HS as a regulator of articular cartilage homeostasis, the results should be interpreted considering the following limitations: First, while the combined study of several mouse lines strongly supports a protective effect of reduced HS level or modification, the investigated mouse mutants, especially the *Col2-Cre;Ndst1*<sup>fl/fl</sup> mutants, show only a modest decrease in OA. Second, we investigated female mice and used the contralateral knee for the sham operation. Due to the higher susceptibility of males for OA and the potentially shift in weight bearing to the sham-operated leg this might lead to an underestimation of the effect of HS on OA severity. Third, the investigation of aggrecan degradation is based on limited sample numbers and the exact mechanism by which protease activity is reduced has still to be deciphered. Fourth, OA was investigated in genetic mouse models likely leading to a developmentally altered articular cartilage quality. The consequences of modifying HS function during OA progression have therefore to be clarified in future studies. Nevertheless, together with the recently published human data<sup>47</sup>, our results support a role of the HS structure in determining the quality of the articular cartilage at multiple levels including cartilage thickness, ECM composition and the activity of proteases, and identify HS as a promising target for future therapies.

## Supplementary Material

Refer to Web version on PubMed Central for supplementary material.

## Acknowledgement

We thank the members of the animal facility for excellent mouse husbandry.

## Role of the funding source

The project was funded by the DFG grants Vo620/10 and Vo620/14 to AV and FOR2722 to BB.

## References

1. Troeberg L, Nagase H. Proteases involved in cartilage matrix degradation in osteoarthritis. *Biochim Biophys Acta*2012;1824:133–45. [PubMed: 21777704]
2. Bishop JR, Schuksz M, Esko JD. Heparan sulphate proteoglycans fine-tune mammalian physiology. *Nature*2007;446:1030–7. [PubMed: 17460664]
3. Yan D, Lin X. Shaping morphogen gradients by proteoglycans. *Cold Spring Harbor Perspectives in Biology*2009;1. a002493–a002493. [PubMed: 20066107]
4. Sarrazin S, Lamanna WC, Esko JD. Heparan sulfate proteoglycans. *Cold Spring Harb Perspect Biol*2011;3.
5. Lin X, Wei G, Shi Z, Dryer L, Esko JD, Wells DE, et al. Disruption of gastrulation and heparan sulfate biosynthesis in EXT1-deficient mice. *Dev Biol*2000;224:299–311. [PubMed: 10926768]
6. Jones KB, Piombo V, Searby C, Kurriger G, Yang B, Grubbs F, et al. A mouse model of osteochondromagenesis from clonal inactivation of Ext1 in chondrocytes. *Proc Natl Acad Sci U S A*2010;107:2054–9. [PubMed: 20080592]
7. Ahn J, Lüdecke H-J, Lindow S, Horton WA, Lee B, Wagner MJ, et al. Cloning of the putative tumour suppressor gene for hereditary multiple exostoses (EXT1). *Nat Genet*1995;11: 137–43. [PubMed: 7550340]
8. Stickens D, Zak BM, Rougier N, Esko JD, Werb Z. Mice deficient in Ext2 lack heparan sulfate and develop exostoses. *Development*2005;132:5055–68. [PubMed: 16236767]
9. Matsumoto Y, Matsumoto K, Irie F, Fukushi J, Stallcup WB, Yamaguchi Y. Conditional ablation of the heparan sulfate-synthesizing enzyme Ext1 leads to dysregulation of bone morphogenic protein signaling and severe skeletal defects. *J Biol Chem*2010;285:19227–34. [PubMed: 20404326]
10. Piombo V, Jochmann K, Hoffmann D, Wuelling M, Vortkamp A. Signaling systems affecting the severity of multiple osteochondromas. *Bone*2018;111:71–81. [PubMed: 29545125]
11. Sgariglia F, Candela ME, Huegel J, Jacenko O, Koyama E, Yamaguchi Y, et al. Epiphyseal abnormalities, trabecular bone loss and articular chondrocyte hypertrophy develop in the long bones of postnatal Ext1-deficient mice. *Bone*2013;57: 220–31. [PubMed: 23958822]
12. Vignon E, Arlot M, Hartmann D, Moyon B, Ville G. Hypertrophic repair of articular cartilage in experimental osteoarthritis. *Ann Rheum Dis*1983;42:82–8. [PubMed: 6830328]
13. von der Mark K, Kirsch T, Nerlich A, Kuss A, Weseloh G, Glückert K, et al. Type X collagen synthesis in human osteoarthritic cartilage. *Arthritis Rheum*1992;35:806–11. [PubMed: 1622419]
14. Pfander D, Swoboda B, Kirsch T. Expression of early and late differentiation markers (proliferating cell nuclear antigen, syndecan-3, annexin VI, and alkaline phosphatase) by human osteoarthritic chondrocytes. *Am J Pathol*2001;159:1777–83. [PubMed: 11696438]
15. Grobe K, Inatani M, Pallerla SR, Castagnola J, Yamaguchi Y, Esko JD. Cerebral hypoplasia and craniofacial defects in mice lacking heparan sulfate Ndst1 gene function. *Development*2005;132:3777–86. [PubMed: 16020517]
16. Pallerla SR, Pan Y, Zhang X, Esko JD, Grobe K. Heparan sulfate Ndst1 gene function variably regulates multiple signaling pathways during mouse development. *Dev Dynam*2007;236: 556–63.
17. Soriano P. Generalized lacZ expression with the ROSA26 Cre reporter strain. *Nat Genet*1999;21:70–1. [PubMed: 9916792]
18. Logan M, Martin JF, Nagy A, Lobe C, Olson EN, Tabin CJ. Expression of Cre Recombinase in the developing mouse limb bud driven by a Prxl enhancer. *Genesis*2002;33:77–80. [PubMed: 12112875]
19. Terpstra L, Prud'homme J, Arabian A, Takeda S, Karsenty G, Dedhar S, et al. Reduced chondrocyte proliferation and chondrodysplasia in mice lacking the integrin-linked kinase in chondrocytes. *J Cell Biol*2003;162:139–48. [PubMed: 12835312]
20. Pond MJ, Nuki G. Experimentally-induced osteoarthritis in the dog. *Ann Rheum Dis*1973;387–8. [PubMed: 4726075]
21. Kamekura S, Hoshi K, Shimoaka T, Chung U, Chikuda H, Yamada T, et al. Osteoarthritis development in novel experimental mouse models induced by knee joint instability. *Osteoarthritis Cartilage*2005;13:632–41. [PubMed: 15896985]

22. Glasson SS, Chambers MG, Van Den Berg WB, Little CB. The OARSI histopathology initiative - recommendations for histological assessments of osteoarthritis in the mouse. *Osteoarthritis Cartilage*2010;18(Suppl 3):S17–23.
23. Schneider CA, Rasband WS, Eliceiri KW. NIH Image to ImageJ: 25 years of image analysis. *Nat Methods*2012;9:671–5. [PubMed: 22930834]
24. Holzer T, Probst K, Etich J, Auler M, Georgieva VS, Bluhm B, et al. Respiratory chain inactivation links cartilage-mediated growth retardation to mitochondrial diseases. *J Cell Biol*2019;218:1853–70. [PubMed: 31085560]
25. Stanton H, Golub SB, Rogerson FM, Last K, Little CB, Fosang AJ. Investigating ADAMTS-mediated aggrecanolysis in mouse cartilage. *Nat Protoc*2011;6:388. [PubMed: 21372818]
26. Fosang AJ, Last K, Maciewicz RA. Aggrecan is degraded by matrix metalloproteinases in human arthritis. Evidence that matrix metalloproteinase and aggrecanase activities can be independent. *J Clin Invest*1996;98:2292–9. [PubMed: 8941646]
27. Woessner JF Jr. Quantification of matrix metalloproteinases in tissue samples. *Methods Enzymol*1995;248:510–28. [PubMed: 7674942]
28. Gelman AC, Stern JB, Dunson HS, Vehtari DB, Rubin DBA. *Bayesian Data Analysis*. 3rd edn. Edition. Taylor & Francis; 2013.
29. Koch AL. Logarithm in biology .1. Mechanisms generating log-normal distribution exactly. *J Theor Biol*1966;12:276–&. [PubMed: 5972197]
30. Muth C, Oravecz Z, Gabry J. User-friendly Bayesian regression modeling: a tutorial with rstanarm and shinystan. *Quant Methods Psychol*2018;14:99–119.
31. Vehtari A, Gelman A, Gabry J. Practical Bayesian model evaluation using leave-one-out cross-validation and WAIC (vol 27, pg 1413, 2017). *Stat Comput*2017;27. 1433–1433.
32. Martel-Pelletier J, Welsch DJ, Pelletier JP. Metalloproteinases and inhibitors in arthritic diseases. *Best Pract Res Clin Rheumatol*2001;15:805–29. [PubMed: 11812023]
33. Zeng GQ, Chen AB, Li W, Song JH, Gao CY. High MMP-1, MMP-2, and MMP-9 protein levels in osteoarthritis. *Genet Mol Res*2015;14:14811–22. [PubMed: 26600542]
34. Little CB, Meeker CT, Fosang AJ. Degradative mechanisms in mouse articular cartilage: use of in vitro models to analyse proteolysis and loss of aggrecan and link protein. *Trans Orthop Res Soc*2003;28:699.
35. Brew K, Nagase H. The tissue inhibitors of metalloproteinases (TIMPs): an ancient family with structural and functional diversity. *Biochim Biophys Acta*2010;1803:55–71. [PubMed: 20080133]
36. Singer II, Kawka DW, Bayne EK, Donatelli SA, Weidner JR, Williams HR, et al. VDIPEN, a metalloproteinase-generated neopeptide, is induced and immunolocalized in articular cartilage during inflammatory arthritis. *J Clin Invest*1995;95: 2178–86. [PubMed: 7537757]
37. Lark MW, Gordy JT, Weidner JR, Ayala J, Kimura JH, Williams HR, et al. Cell-mediated catabolism of aggrecan. *J Biol Chem*1995;270:2550–6. [PubMed: 7852317]
38. Makowski GS, Ramsby ML. Calibrating gelatin zymograms with human gelatinase standards. *Anal Biochem*1995;236: 353–6.
39. Troeberg L, Nagase H. Zymography of metalloproteinases. *Curr Protocols Protein Sci*2003;33. 21.15.21–21.15.12.
40. Ogata Y, Enghild J, Nagase H. Matrix metalloproteinase 3 (stromelysin) activates the precursor for the human matrix metalloproteinase 9. *J Biol Chem*1992;267:3581–4. [PubMed: 1371271]
41. Van Hul M, Lijnen HR. A functional role of gelatinase A in the development of nutritionally induced obesity in mice. *J Thromb Haemostasis*2008;6:1198–206. [PubMed: 18433461]
42. Echtermeyer F, Bertrand J, Dreier R, Meinecke I, Neugebauer K, Fuerst M, et al. Syndecan-4 regulates ADAMTS-5 activation and cartilage breakdown in osteoarthritis. *Nat Med*2009;15: 1072–6. [PubMed: 19684582]
43. Shu CC, Jackson MT, Smith MM, Smith SM, Penm S, Lord MS, et al. Ablation of perlecan domain 1 heparan sulfate reduces progressive cartilage degradation, synovitis, and osteophyte size in a preclinical model of posttraumatic osteoarthritis. *Arthritis Rheum*2016;68:868–79.

44. Kaneko H, Ishijima M, Futami I, Tomikawa-Ichikawa N, Kosaki K, Sadatsuki R, et al. Synovial perlecan is required for osteophyte formation in knee osteoarthritis. *Matrix Biol*2013;32:178–87. [PubMed: 23339896]
45. Otsuki S, Hanson SR, Miyaki S, Grogan SP, Kinoshita M, Asahara H, et al. Extracellular sulfatases support cartilage homeostasis by regulating BMP and FGF signaling pathways. *Proc Natl Acad Sci U S A*2010;107:10202–7. [PubMed: 20479257]
46. Otsuki S, Murakami T, Okamoto Y, Hoshiyama Y, Oda S, Neo M. Suppression of cartilage degeneration by intra-articular injection of heparan sulfate 6-O endosulfatase in a mouse osteoarthritis model. *Histol Histopathol*2017;32:725–33. [PubMed: 27808352]
47. Chanalaris A, Clarke H, Guimond SE, Vincent TL, Turnbull JE, Troeberg L. Heparan sulfate proteoglycan synthesis is dysregulated in human osteoarthritic cartilage. *Am J Pathol*2019;189:632–47. [PubMed: 30553836]
48. Ruiz-Gomez G, Vogel S, Moller S, Pisabarro MT, Hempel U. Glycosaminoglycans influence enzyme activity of MMP2 and MMP2/TIMP3 complex formation - insights at cellular and molecular level. *Sci Rep*2019;9:4905. [PubMed: 30894640]
49. Sato H, Takino T, Okada Y, Cao J, Shinagawa A, Yamamoto E, et al. A matrix metalloproteinase expressed on the surface of invasive tumour cells. *Nature*1994;370:61–5. [PubMed: 8015608]
50. Fridman R, Toth M, Pena D, Mobashery S. Activation of progelatinase B (MMP-9) by gelatinase A (MMP-2). *Canc Res*1995;55:2548–55.
51. Yamamoto K, Murphy G, Troeberg L. Extracellular regulation of metalloproteinases. *Matrix Biol*2015;44–46:255–63.
52. Schuksz M, Fuster MM, Brown JR, Crawford BE, Ditto DP, Lawrence R, et al. Surfen, a small molecule antagonist of heparan sulfate. *Proc Natl Acad Sci U S A*2008;105:13075–80. [PubMed: 18725627]
53. Huegel J, Mundy C, Sgariglia F, Nygren P, Billings PC, Yamaguchi Y, et al. Perichondrium phenotype and border function are regulated by Ext1 and heparan sulfate in developing long bones: a mechanism likely deranged in Hereditary Multiple Exostoses. *Dev Biol*2013;377:100–12. [PubMed: 23458899]
54. Huegel J, Enomoto-Iwamoto M, Sgariglia F, Koyama E, Pacifici M. Heparanase stimulates chondrogenesis and is up-regulated in human ectopic cartilage: a mechanism possibly involved in hereditary multiple exostoses. *Am J Pathol*2015;185:1676–85. [PubMed: 25863260]
55. Bachvarova V, Dierker T, Esko J, Hoffmann D, Kjellen L, Vortkamp A. Chondrocytes respond to an altered heparan sulfate composition with distinct changes of heparan sulfate structure and increased levels of chondroitin sulfate. *Matrix Biol*2020, 10.1016/j.matbio.2020.03.006.



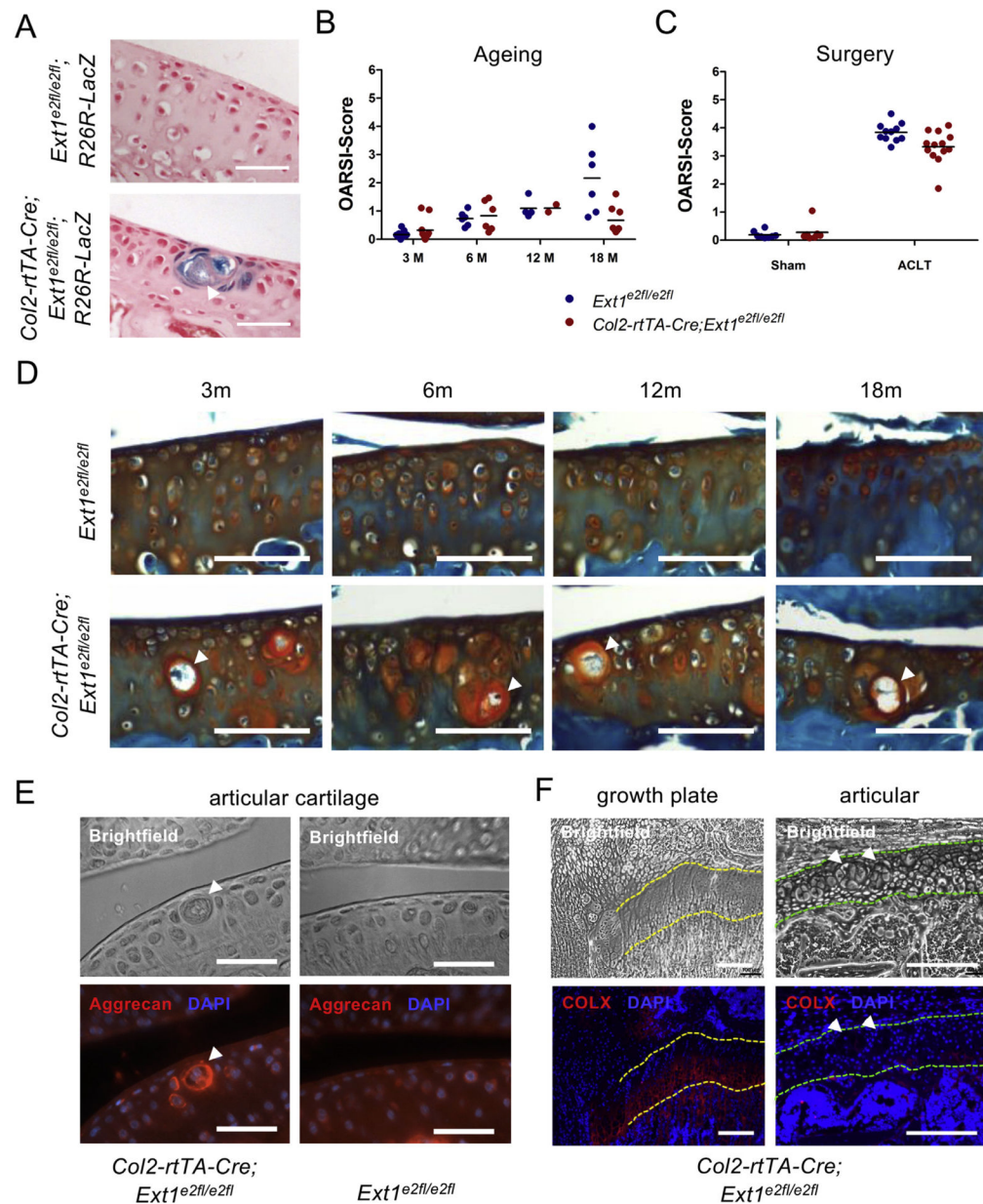


**Fig. 1. Clonal deletion of *Ext1* in *Col2-rtTA-Cre;Ext1<sup>e2fl/e2fl</sup>* mice protects against OA**  
 (A) Cre activity in 6 week old *Col2-rtTA-Cre;Ext1<sup>e2fl/e2fl</sup>;R26R-LacZ* samples was detected by β-Galactosidase staining of sagittal sections. Recombined cells are clustered and enlarged in size. Doxycycline administration at P8. Scale Bar: 50 μm; counterstaining: Nuclear Fast Red. White arrow head indicates cluster of recombined cells. (B) OARSI scores of *Ext1<sup>e2fl/e2fl</sup>* and *Col2-rtTA-Cre;Ext1<sup>e2fl/e2fl</sup>* mice, black line indicates mean. OA scores increase over time in both genotypes. At 18 months *Col2-rtTA-Cre;Ext1<sup>e2fl/e2fl</sup>* animals display reduced OA scores compared to *Ext1<sup>e2fl/e2fl</sup>* littermates (3m: *n* = 11, 6m: *n* = 6, 12m: *n* = 2, 18m: *n* = 6). Effect sizes: genotype 0.49 (95% HDI -0.27–1.25), age 0.13 (95% HDI 0.08–0.18), genotype and age 0.09 (95% HDI -0.16 to -0.03). Doxycycline administration at P8, analysis at 3, 6, 12 and 18 months. (C) OARSI scores of wildtype



and *Col2-rtTA-Cre;Ext1<sup>e2fl/e2fl</sup>* mice after surgery. *Col2-rtTA-Cre;Ext1<sup>e2fl/e2fl</sup>* mice show reduced OA scores after ACLT (M: ACLT  $n = 13$ , sham  $n = 7$ ; WT: ACLT  $n = 11$ , sham  $n = 8$ ). Effect size: 0.83 (95% HDI 0.72–0.96). Doxycycline administration at 6 weeks, ACLT at 8 weeks, analysis at 12 weeks. (D) Safranin-O staining of frontal sections through knee joints of wildtype and *Col2-rtTA-Cre;Ext1<sup>e2fl/e2fl</sup>* mice at 3, 6, 12, and 18 months of age reveals decreased cartilage erosion in *Col2-rtTA-Cre;Ext1<sup>e2fl/e2fl</sup>* animals. Clusters of enlarged cells are present at all analyzed timepoints. Doxycycline administration at P8. Scale bar: 100  $\mu\text{m}$ . White arrow heads indicate clusters of recombined cells. (E, F) Immunofluorescence labeling of aggrecan (E) and COLX (F) on sagittal sections of 4 weeks old *Col2-rtTA-Cre;Ext1<sup>e2fl/e2fl</sup>* mice. Increased aggrecan levels surround clusters of mutant cells in the articular cartilage. COLX is not expressed in mutant cells of the articular cartilage, while a clear signal is detected in hypertrophic chondrocytes of the growth plate on the same section. Doxycycline administration at P8. Scale Bar E: 50  $\mu\text{m}$ , F: 200  $\mu\text{m}$ . White arrow heads exemplify clusters of recombined cells. Outlines of growth plate (yellow) and articular cartilage (green) are highlighted by dashed lines.

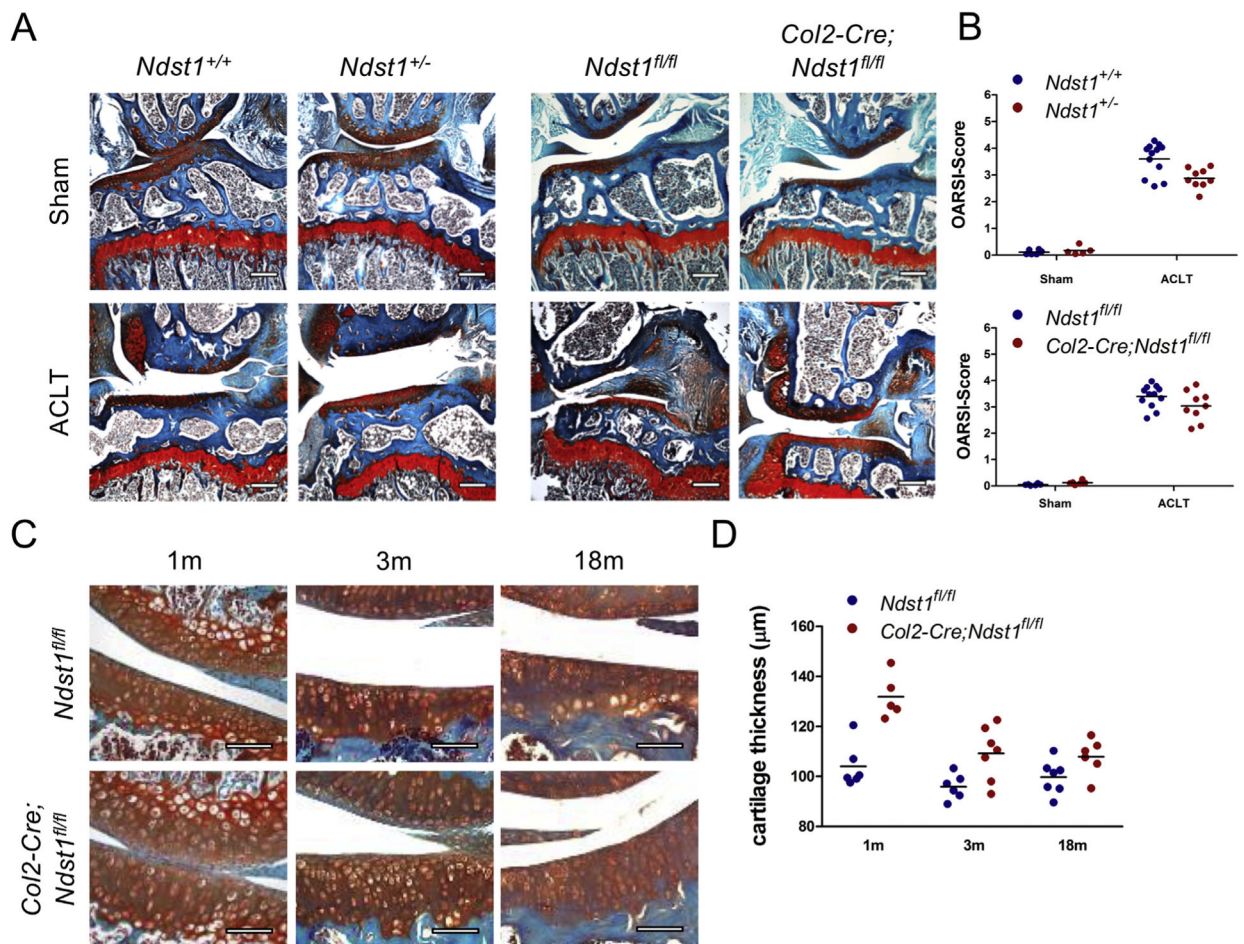


**Fig. 2. *Ndst1*<sup>+/-</sup> and *Col2-Cre;Ndst1*<sup>fl/fl</sup> animals develop less severe OA after ACLT surgery.** (A) Safranin-O staining of frontal sections of knee joints from *Ndst1*<sup>+/+</sup>, *Ndst1*<sup>+/-</sup>, *Ndst1*<sup>fl/fl</sup> and *Col2-Cre;Ndst1*<sup>fl/fl</sup> mice after surgery. Both *Ndst1* mutants display reduced signs of OA compared to wildtype littermates. ACLT surgery at 8 weeks, analysis at 12 weeks. Scale Bar: 200 μm. (B) OA scores of individual mice, black lines indicate mean (*Ndst1*<sup>+/+</sup>: ACLT *n* = 12, sham *n* = 6; *Ndst1*<sup>+/-</sup>: ACLT *n* = 9, sham *n* = 5; *Ndst1*<sup>fl/fl</sup>: ACLT *n* = 12, sham *n* = 6; *Col2-Cre;Ndst1*<sup>fl/fl</sup>: ACLT *n* = 9, sham *n* = 6). OA score change factors associated to mutation: *Ndst1*<sup>+/-</sup> 0.82 (95% HDI 0.74–0.90), *Ndst1*<sup>fl/fl</sup> 0.87 (95% HDI 0.76–1.00). (C) Safranin-O staining of sagittal sections from *Ndst1*<sup>fl/fl</sup> and *Col2-Cre;Ndst1*<sup>fl/fl</sup> mice at 1, 3, and 18 months of age. *Col2-Cre;Ndst1*<sup>fl/fl</sup> mutants display an increased thickness of the articular cartilage. Scale Bar: 100 μm. (D) Quantification of cartilage thickness, black lines indicate mean (1m: *n* = 5, 3m: *n* = 6, 18m: *n* = 6). Thickness change due to mutation: 1.24 (95% HDI 1.15–1.33).

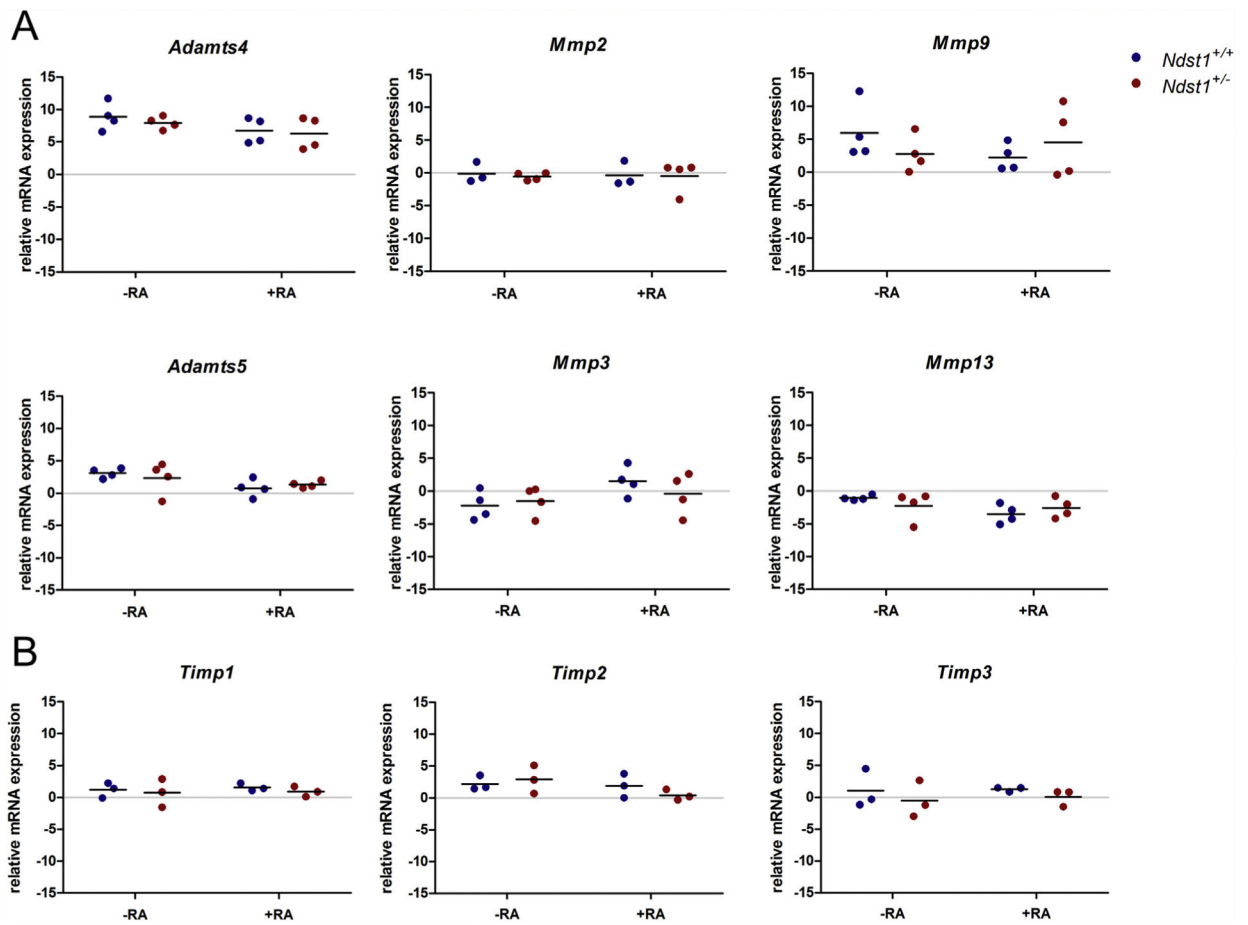


**Fig. 3. The expression levels of major proteases and protease inhibitors are not altered in *Ndst1*<sup>+/-</sup> mice**

qRT-PCR analysis of protease and protease inhibitor expression in femoral heads cultured for 3 days in the presence or absence of RA. Scatter plots display CT values relative to B2M, black lines indicate means (mRNA pools from  $n = 3$  litters; no statistical difference; Tables S3 and S4).

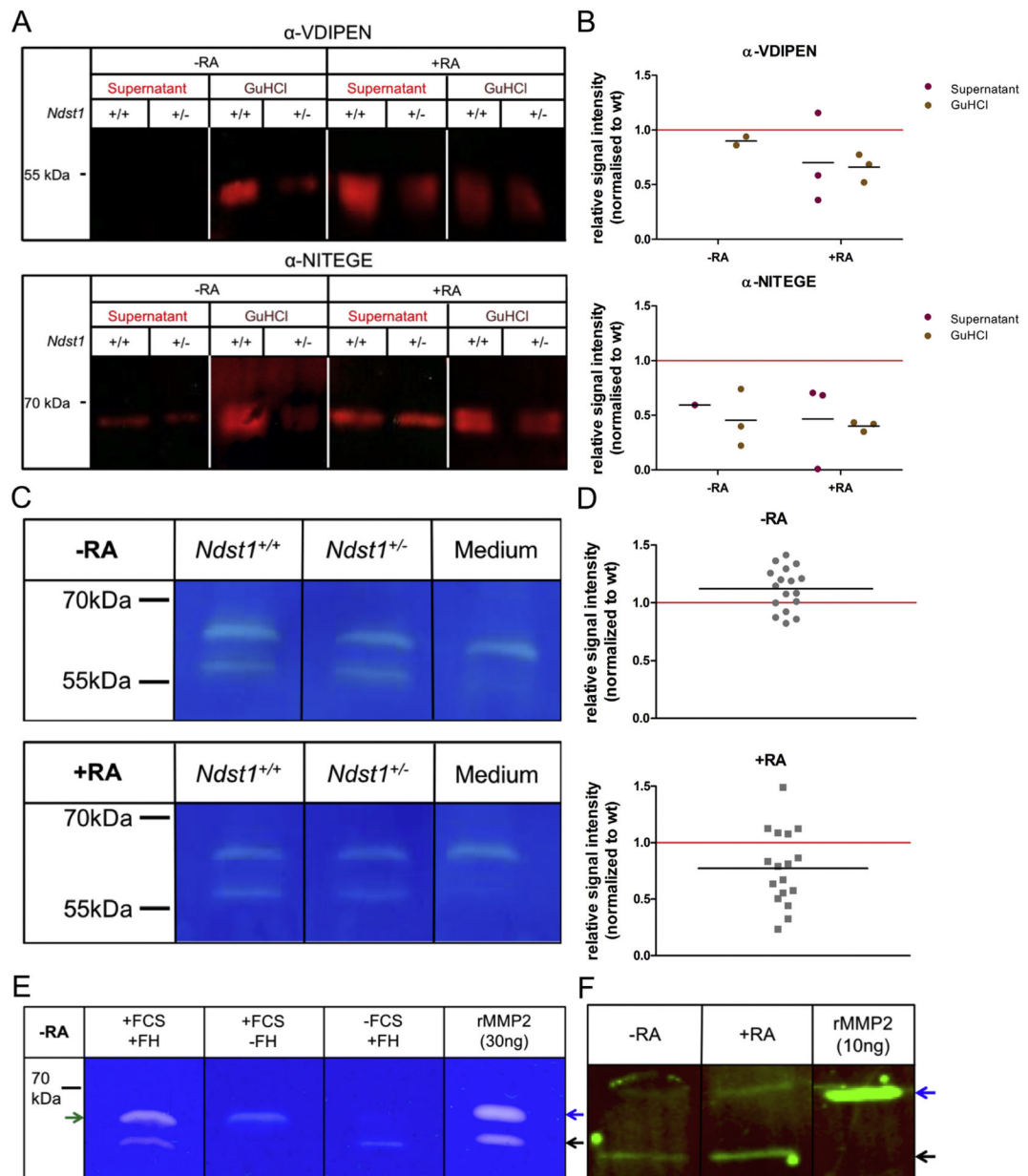


**Fig. 4. Protease activity is reduced in *Ndst1*<sup>+/-</sup> mutants.**

(A) Western Blot analysis of the aggrecan neo-epitopes VDIPEN and NITEGE in supernatants and GuHCl extracts of femoral head explants cultured in the presence or absence of RA. Signal intensities are decreased in RA-treated *Ndst1*<sup>+/-</sup> samples. (B) Scatter plots represent relative values of individual litters (littermates pooled by genotype; *n* = 3 litters, normalized to wildtype (wt)). Wildtype-associated factors of mean increase of digestion signal: NITEGE 4.24 (95% HDI 1.05–18.6), VDIPEN 1.54 (95% HDI 1.00–2.34). (C) Gelatin zymography of supernatants of femoral head explants cultivated with or without RA. A protease of ~65 kDa is contained in the culture medium. At ~58 kDa a femoral head-specific protease is present, which is less active in *Ndst1*<sup>+/-</sup> samples upon RA treatment. (D) Scatter plots represent quantified signal intensities from individual femoral

heads normalized to wildtype (wt), black lines indicate means ( $n = 17$  mice, from 6 litters). Effect size without RA treatment: 1.09 (95% HDI 0.90–1.34), effect size upon RA treatment: 0.77 (95% HDI 0.60–0.96). (E) Gelatin zymography of supernatants of femoral head cultures compared to recombinant mouse/rat MMP2 protein (rMMP2). Black arrow: active MMP2; blue arrow: proMMP2; green arrow: unspecific protease from FCS. (F) Western Blot analysis of MMP2 in the supernatant of femoral head cultures with and without RA treatment. Blue arrow: proMMP2; black arrow: active MMP2 ( $n = 3$ ).

Author Manuscript

Author Manuscript

Author Manuscript

Author Manuscript